

Real-Time Biosensor Platform: Fully Integrated Device for Impedimetric Assays

Andrey L. Ghindilis^a, Kevin R. Schwarzkopf^a, Dean S. Messing^a, Ibrahim Sezan^a, Paul Schuele^a, Changqing Zhan^a, Maria W. Smith^b, Holly M. Simon^b, and David R. Evans^a.

^aSHARP Laboratories of America, Inc., 5700 NW Pacific Rim Blvd, Camas, WA 98607.

^bCenter for Coastal Margin Observation & Prediction and Division of Environmental and Biomolecular Systems, Oregon Health & Science University, 20000 NW Walker Road, Beaverton, OR 97006 USA.

An impedimetric biosensor platform for bio-affinity assays was developed based on real-time, label-free electrochemical detection performed via direct interface to electronic digital data processing. The sensor array consists of 15 gold microelectrode pairs enclosed in three reaction chambers and bio-functionalized with specific DNA probes. The impedance change caused by specific target analyte binding to the functionalized electrode surface is recorded in real time. The detector is capable of continuous and simultaneous stimulation and recording of all array electrodes. A corresponding mathematical algorithm, and a software package for data analysis were developed and used to quantify both the rate of target to probe binding, and target to probe affinity. The biosensor was capable of distinguishing between closely-related bacterial strains. This fully-integrated sensor array platform can be used for detection of a wide range of analytes of practical significance, and has potential for further integration with amplification (i.e. PCR) and sample preparation modules.

Introduction

Impedimetric detection has a number of attractive features for development of affinity biosensors. Detection does not require molecular labeling of a target analyte, which simplifies the sample preparation protocols and reduces the number of steps in the assay workflow. The label-free, real-time detection mode also provides important data on target to probe binding kinetics. Additionally, impedimetric assays can be performed at low cost if instrumentation and arrays are fabricated using the standard monolithic processing. Together, these features are especially beneficial for development of the miniaturized lab-on-the-chip biosensor format.

The described advantages have resulted in a rapidly expanding area of research and development centered on impedimetric biosensors (1-6). However, this rapid development is still somewhat hampered by the absence of a standardized, low-production-cost format that integrates sensor arrays and compatible measuring instrumentation. This lack has effectively limited commercialization of impedimetric biosensors. Creation of such a platform, with the added benefit of full flexibility to cover

a large variety of applications, would facilitate numerous research projects based on impedimetric biosensors. This platform should comprise: (i) multiplexed arrays with sensor surface adaptable for different types of biochemical and chemical functionalization; (ii) an instrument capable of making parallel measurements on multiple electrodes in real time; and (iii) an integrated software package for data analysis and rapid quantification of the real-time data. Development of such a platform has been our goal. Our first prototype contained eight gold interdigitated microelectrodes functionalized with DNA oligonucleotide probes bound to the surface with thiol groups, and was used to develop an assay for detection of bacterial DNA (6). The prototype array signals were detected using Reference 600TM Potentiostat from Gamry Instruments (Warminster, PA). Our goal, however, has been to design and construct a specialized and inexpensive detector at Sharp Laboratories of America (SLA). This Reader has been developed using advanced electronics. It can simultaneously read 16 channels at a high scan rate and contains a software package to perform full analysis of electrode impedance changes obtained in real time mode. In this report, we describe development of the next-generation sensor array and integrated reader platform, and its application for the detection of specific bacterial targets using a nucleic acid assay.

Experiment

Impedimetric micro-array fabrication

Fabrication of sensor microarrays was based on photolithography, followed by 150 nm gold film deposition by E-beam evaporation, and liftoff process. The negative sidewall profile of the photoresist patterns was a key to achieve clean liftoff patterns. A thin layer (30nm) of chrome was first deposited as adhesion layer prior to gold deposition. Both chrome and gold film thicknesses were monitored by a quartz crystal microbalance (QCM) system. Each fabricated array had 15 pairs of electrodes (Fig. 1a,b). The individual impedimetric sensor electrode had a typical dimension of $3350\mu\text{m} \times 100\mu\text{m} \times 150\text{nm}$, and the spacing between the sensor electrode and the common electrode was $40\mu\text{m}$. The size of each die of fabricated impedimetric microarray on 6 inch glass substrate was $20\text{mm} \times 18.5\text{mm}$ (Fig. 1a).

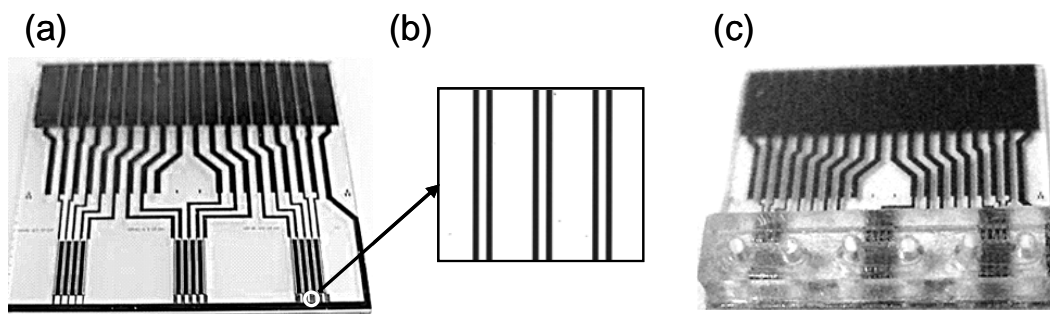


Figure 1. (a) Impedimetric sensor microarray; (b) gold interdigitated microelectrode; (c) ready-to-use sensor array with a microfluidic chamber attached.

The fabricated arrays were electrically tested on wafer level for quality control. The test was based on electrical resistance screening to identify any shorted devices. Qualified

wafers were then diced into dies, and clean procedures using solvent and oxygen plasma were performed before biofunctionalization.

Preparation of oligonucleotide-sulfhydryl solutions and microarray functionalization

The 10 mM solution of commercially synthesized, thiol-modified oligonucleotide (TMO) in deionized water was incubated with 2 mM 1,4-dithiothreitol for approximately 1 hour at ambient temperature, and purified by passing it through two sequential P6 microspin columns (Biorad Laboratories, Hercules, CA). The eluate was diluted 10 times with 8X PBS (phosphate buffered saline) buffer containing 5 mM magnesium chloride and 1 mM Na₂EDTA.

After microarray fabrication the wafer was diced to obtain individual arrays and washed 2 times with acetone and once with isopropyl alcohol. The arrays were then dried by pressurized nitrogen and treated with downstream oxygen plasma. A plastic, triple micro-fluidics chamber having six solution portals was then fixed over the array with adhesive. The fluidics chamber contained three separated cells of 23 μ L volume, each enclosing five electrode pairs (Fig. 1c). Thus, a single array can be used for three independent assays. Oligonucleotide-sulfhydryl containing solution was added to each cell. The array was incubated for 4 hours at ambient temperature, washed with DI water, dried and stored at room temperature. Prior to use, the array was treated with 10 mM solution of sodium hydroxide for 10 min, washed with DI water, and incubated with a working buffer solution for > two hours.

Quality control of functionalized arrays using fluorescent beads

Each 5th or 10th randomly selected array of a functionalized set was tested for quality in the following manner: The biotinylated oligonucleotide target complementary to the array probes (500 nM solution in 1X PBS with 0.05% Tween 20 [PBST]) was added to cell 1 of the tested arrays. A biotinylated non-target oligonucleotide (500 nM in PBST, with a sequence that was not complementary to the array probes) was added to cell 2, and target-free PBST was added to cell 3. The array was then incubated for 45 minutes at ambient temperature and washed with PBST. Then a suspension (1:1000 dilution in PBST) of the avidin-modified fluoro-beads (FluoSpheres® NeutrAvidin® labeled microspheres, Invitrogen, Carlsbad, CA) was added to all cells of the array followed by incubation for 30 minutes at ambient temperature. After incubation, the microfluidic 3-cell chamber was removed from the array, and the microelectrode surface was washed with PBST, and examined under a fluorescent microscope. This testing provided information on ability of the electrode surface to bind nucleic acids specifically and non-specifically. If the testing showed good specific binding in cell 1, minimum non-specific binding in cell 2, and low overall background in cell 3, the microarray batch passed the quality control test.

Preparation of DNA targets and oligonucleotide array probes

Escherichia coli strains, target genes, PCR primers for amplification of DNA targets, annealing temperatures and sizes of the corresponding DNA amplicons are shown in Table 1. Primer sequences and PCR conditions have been described previously (9-11).

Table 1. Target *E. coli* genes, strains, and PCR primers used for amplification of target DNA fragments.

| Gene | <i>E. coli</i> strain | Primer name | Primer sequence | T (°C)* | Product (bp) |
|------|-----------------------|------------------|-----------------------------|---------|--------------|
| adk | MG1655 | Forward: adkF | 5'-ATTCTGCTTGGCGCTCCGGG-3' | 60 | 193 |
| | CFT073 | Reverse: adkR | 5'-CCAGCGGATCACCAGTTCG-3' | | |
| hlyA | CFT073 | Forward:HlyA-F16 | 5' CAGTCCTCATTACCCAGCAAC 3' | 60 | 355 |
| | | Reverse:HlyA-B14 | 5' ACAGACCCCTTGTCTGAAC 3' | | |
| stx2 | EDL 933 | Forward: GK5 | 5'-ATGAAGAAGATGTTTATG-3' | 50 | 269 |
| | | Reverse: GK6 | 5'-TCAGTCATT ATTAAACTG-3' | | |

* Annealing temperature (°C) used for PCR amplification.

All oligonucleotides were purchased from Integrated DNA Technologies (Skokie, IL). For some applications, the forward primers contained a biotin label at the 5' end, which became incorporated into the sense strand of the double-stranded PCR product. Purified bacterial genomic DNA was purchased from ATCC® (<http://www.atcc.org/>). PCR was performed according to the following: one cycle of denaturation at 94°C for 2 min, followed by 40 cycles of denaturation at 94°C for 30 sec, annealing at 60°C (50°C for stx2) for 30 sec, and extension at 72°C for 1 min, with the final extension step at 72°C for 7 min. PCR products were analyzed by gel electrophoresis and purified using the Wizard PCR purification system (Promega Corp., Madison, WI).

Oligonucleotide probes used for functionalization of sensor arrays are shown in Table 2. These were modified with thiol groups (TMO) from either the 3' or 5'-end. Each TMO probe was used for the functionalization of several batches of sensor microarrays from different fabrication lots.

Table 2. Oligonucleotide probe sequences used for sensor functionalization.

| Gene of interest | Probe sequence |
|------------------|-----------------------------|
| adk | 5'- TGGAGAAATATGGTATTCCG-3' |
| hlyA | 5'- GCGGTTTTATTTGCATTAGT-3' |
| stx2 | 5'- TGAATTCCAGAAGCAAGTCT-3' |

Impedimetric assay

The detection principle employed was based on electrochemical impedance spectroscopy. It involved application of a small sinusoidal voltage, an input waveform of 100-150 mV magnitude at 100-150 Hz frequency, and measurement of the resulting current flow. The data presented in this study were obtained at 100 Hz 100 mV for *E. coli* DNA detection and at 150 Hz 150 mV for oligonucleotide detection. The measured current-to-voltage ratio provided the Z value of complex surface impedance in Ohm. The Z value changed when target hybridization increased the charge density near the electrode surface due to the addition of the negatively charged DNA phosphate backbone.

Prior to measurement of target-probe interactions, a sensor microarray was inserted into the Reader, the microfluidic chamber was filled with target-free buffer, and detection was performed for 10-15 minutes to establish and stabilize the baseline. The target-free buffer solution was subsequently replaced with additional buffer supplemented with

target at specified concentrations. We used SSPE (containing 150 mM sodium chloride, 10 mM sodium phosphate, and 10 mM Na₂EDTA) buffer for DNA amplicon targets, and supplemented with 0.05% Tween 20 (SSPET) for oligonucleotide targets.

Double-stranded DNA targets were denatured by incubation at 95°C for five minutes immediately prior to injection into the microfluidic cell. After target injection, change of the electrode pair impedance was detected in real time mode, followed by data analysis. Target-probe hybridization was performed at 37°C and 47°C, for oligonucleotide and DNA amplicon targets, respectively.

Results and Discussion

Development of the impedimetric instrumentation

Impedance spectroscopy biosensing is based on detection of electrical properties, *viz.*, magnitude and phase relations between voltage drop across and current flowing through the sensing device, as a function of AC input signal frequency. Measurements can be made in the form of scans of impedance in the frequency domain, or determination of impedance variation in the time domain at one or more fixed frequencies, etc. Impedance spectroscopic techniques are very flexible, and, because they are based on electronics, do not require expensive optical sources, detectors, and fluorescent reagents. Physically, impedance changes are caused by material changes in the near-surface environment of the electrode and, thus, provide a direct means of detecting target-probe binding reactions on the sensor. Concomitantly, sensor response is generally proportional to the amount of captured target. Accordingly, the assay is a direct, single-stage procedure and can be performed in real-time to measure the kinetics of the interaction as well.

Early in the course of this project we found that commercially available impedance spectroscopy instruments were not capable of performing multiplexed measurements and, moreover, had fundamental limitations regarding access and manipulation of raw electrical signals. This was not due to any inherent problem, but rather because of their generalized applicability to a wide variety of electrochemical measurements. A first-generation specialized electronic system was designed and fabricated based on a Reference 600TM Potentiostat from Gamry Instruments (Warminster, PA) accompanied with a multiplexor and temperature controller designed at SLA (6). This design was found to have some limitations, thus a semi-custom second-generation system was designed and fabricated. This second generation system allowed sequential measurement of eight array electrodes and exported the data to a custom, in-house software package resident on an associated computer through a standard USB interface. Based on results obtained from the second-generation system, a third-generation system optimized for low noise and constant stimulation of all sensors was designed and fabricated. The resultant instrument had the following characteristics: (i) stimulation voltage range was 0-212 mV; (ii) stimulation frequency range was 10-3000 Hz; (iii) load impedance was up to 500K ohms; (iv) high scan rate of eight impedance measurements per second per channel; (v) sensor temperature control; (vi) ethernet connection to host computer; and (vii) ability to scan 16 channels simultaneously. The instrument photo can be seen at <http://www.sharplabs.com/docs/CMOP-SLA.pdf>

Data analysis algorithm

Surface chemistry theory suggests that target molecules bind to the immobilized probe layer at a rate that obeys an exponential function. This rate decreases with time after the target is injected into the reaction chamber. Thus, electrode impedance also varies (approximately) as a function of time, or sample index n in the discrete-time case, and is well-modeled by

$$|Z(t)| = B + A(1 - e^{-st}) + v(t) \quad [1]$$

where s , A , and B are non-negative constants. Here, B is the offset at which the exponential begins, and represents the biosensor baseline impedance of the target-free buffer solution. The noise inherent in every biosensor is represented by v . Both s and A hold important biochemical information. The former expresses the decay time constant and closely tracks the concentration of the analyte. The latter is correlated to the sensor surface coverage which relates to the molecular affinity of target-probe interactions.

The main difficulties in estimating the parameters of Equation [1] are the substantial additive noise present in the signal and the non-linear involvement of s . We investigated methods for performing non-linear estimation that belong to an algorithm class having several common features. First, it assumes a general signal model that is composed of uniformly spaced samples of a sum of M complex exponentials corrupted by zero-mean Gaussian noise, $v(n)$, and observed over a time aperture of N samples. This is described by the formula

$$y(n) = \sum_{k=1}^M a_k e^{\beta_k n} + v(n) \quad n = 0, 1, \dots, N-1 \quad [2]$$

The $\{\beta_k\}$ are called the *complex frequencies* or *poles* of the signal and $\{a_k\}$ are the complex amplitudes. Here $\beta_k = -\alpha_k + j2\pi f_k$ are complex numbers (α_k is non-negative). $\{\alpha_k\}$ are the pole damping factors and $\{f_k\}$ are the pole frequencies. It is clear that Equation [1] is a special case of Equation [2], with two real poles (one of which at the origin of the complex plane) and real-valued amplitudes ($B + A$) and $-A$.

Second, the non-linear problem is broken into two steps (7). Step 1 uses the *linear prediction* property,

$$y(n) = \sum_{k=1}^M c_k y(n-k) \text{ of Equation [2] (with } v = 0) \quad [3]$$

to perform the simpler task of estimating the parameters of a related linear model. Step 2 then extracts the non-linear parameters from the linear model. The last common feature is that Step 1 employs a low dimensional subspace projection of the matrix associated with the linear model to reduce the effects of noise. Two algorithm families within this class were investigated. The first family is typified by the Kumarisan-Tufts method described in (8). In these approaches, Step 1 designs an adaptive (linear) filter that nulls any input signal of the form of Equation [2]. Step 2 extracts the zeros of the filter polynomial and computes the $\{\beta_k\}$ via algebraic manipulation of each zero. Following this, a scheme such as *Total Least Squares* is used on the partial model to estimate the $\{a_k\}$. The second family of approaches uses a state-space representation for the linear model. Step 1 uses

the input data to estimate the parameters of the state-feedback matrix associated with a related linear model. In Step 2 the eigenvalues of the matrix are computed. These contain the system poles of Equation [2]. The remainder of Step 2 (estimating the $\{a_k\}$) is as above. A promising technique was found in a state-space algorithm for NMR signal processing described in Fotinea et al. (12).

Figure 2. Graphical representation of parameters A and s.

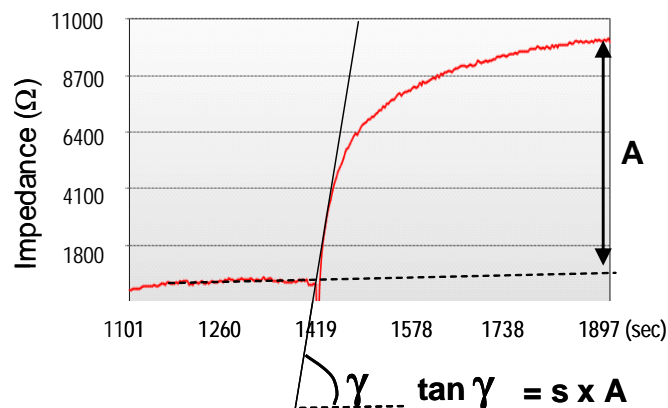


Figure 2 depicts a direct graphical interpretation of parameter A for an impedance response obtained for oligonucleotide target binding detection. Parameter A represents the ‘end point’ of the binding curve (with baseline B subtracted out). This parameter combines several characteristics of the binding event: density of the formed layer of the bound target molecules, size of the target molecules, and dielectric property of the target molecules. Fig. 2 also indirectly indicates how parameter s (the time constant of the underlying exponential function) enters into a commonly measured quantity, i.e. the initial slope of the curve. In order to obtain parameter s in this way one would need to divide the initial slope by the end-point measured value of A. Both measurements contain errors which combine to make s (obtained in this way) quite inaccurate.

The developed algorithm allows one to extract parameters A and s *separately*. Furthermore the algorithm estimates s without needing A so errors in A do not affect parameter s. In addition, the algorithm can estimate both A and s from just the initial portion of the impedance record so one does not need to wait to make an endpoint measurement to obtain A. Of course, the more data that is given to the algorithm, the more accurate the parameter estimates tends to be.

For comparative quantification of binding of different concentrations of the same target molecule, parameter s alone may be used. However, to compare binding characteristics of closely related targets, such as mutant *vs* wild-type DNA, or DNA targets with the same binding sequence but different molecular sizes, both parameters A and s have to be taken into account separately. A combination of parameters A and s provide a signature of the binding event and allows one to obtain a comprehensive characteristic of probe-target binding behavior.

Oligonucleotide detection

Application of a short oligonucleotide target as a model analyte for the impedimetric assay is widely used to estimate assay performance, such as specificity and dynamic range. We used 20-mer and 35-mer oligonucleotide targets that were complementary (antisense) to sensor microarray probes. Binding of targets to the corresponding probes

caused an increase in surface density of biomolecules (the surface layer thickness did not change), and resulted in a change of impedance (signal response).

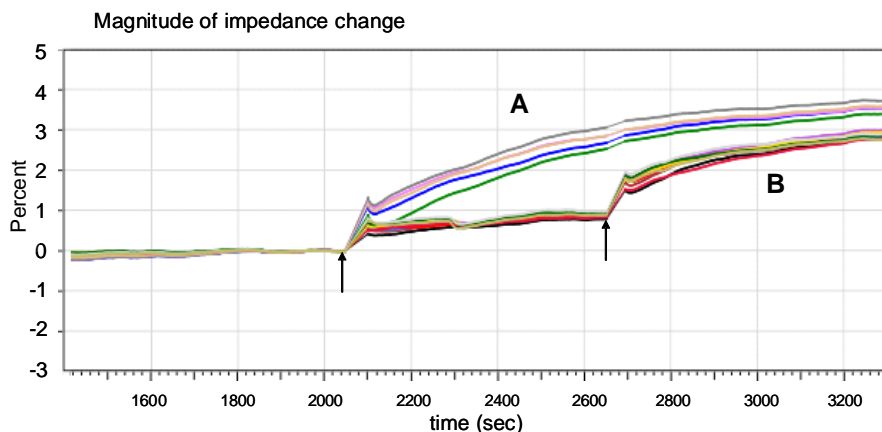


Figure 3. Impedance response detected in two microfluidic cells (each with 5 electrodes) after injection of 20-mer oligonucleotide targets (at 500 nM concentrations). Cell A, injection of targets complementary to the electrode probes; Cell B, first injection of non-target oligonucleotides, followed by injection of complementary targets. Arrows indicate sample injection times.

Figure 3 shows the impedance change expressed as percentage of the initial impedance value obtained for 10 electrodes in two cells. Cell A was directly injected with targets complementary to the electrode probes, whereas cell B was first injected with non-target oligonucleotides (negative control), and then with the complementary ones. Significant increase of electrode impedance was observed for injection of complementary targets. In contrast, the negative control injection resulted in an insignificant increase in electrode impedance.

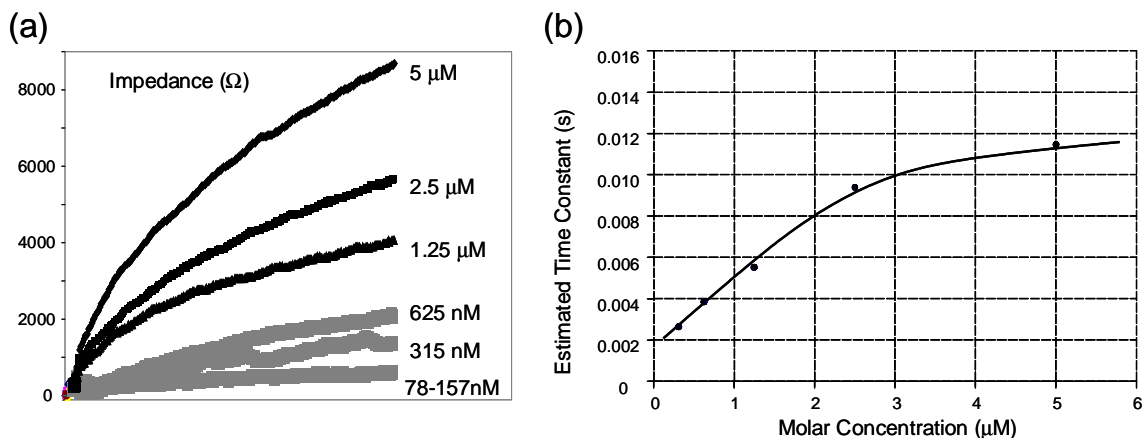


Figure 4. (a) Impedance response to different concentrations of complementary oligonucleotides; (b) Dependence of the parameter s (the rate of binding (Fig. 2)) on the oligonucleotide target concentrations.

Dependence of the impedance response on concentrations of the target 35-mer oligonucleotide (5'-AAA CAA CTA GCA ATG GCA TTT CGC ACT ACC-3') is shown

in Figure 4a. The rate of binding s extracted for these plots (as in Equation [1]) is linear within a concentration range of 78 nM to 2.5 μ M (Fig. 4b). This linear dependence of the parameter s on the target concentration also confirms that it can be used to generate calibration plots using the developed data analysis algorithm.

Bacterial DNA detection

To demonstrate applicability of the developed impedimetric platform for detection of genomic DNA of microorganisms we used *Escherichia coli* genomic DNA as a model analyte. Several genes were selected as targets, including adenylate kinase (*adk*) gene from the established multi-locus sequence tag (MLST) gene set (9) that is used for general detection of *E. coli*. Two other genes of interest were selected from known markers of virulence in *E. coli* strains. One of them, Shiga toxin 2 (*stx2*) is an indicator for severe clinical outcome in infected patients (10), and another one, α -hemolysin gene (*hlyA*) is widely present in enterohaemorrhagic (EHEC) and enteropathogenic (EPEC) strains (11). These genes are widely used in PCR-based *E. coli* detection strategies, and the corresponding PCR primers and amplification conditions have been well established (10,11). Three *E. coli* strains were used for detection: commensal K-12 isolate MG1655 (*adk* gene only), enterohemorrhagic strain EDL933 O157:H7 (*adk*, *stx2*), and uropathogenic clinical strain CFT073 (*adk*, *hlyA*). The array probes corresponding to *adk*, *hlyA* and *stx2* genes were designed from the sequences of DNA fragments positioned in the middle of the amplicons. The following criteria were used for probe design: (i) 20-mer length; (ii) hybridization T_m approximately 55°C; and (iii) no hairpin structure formation (positive $\Delta^\circ G$ and $T_m \leq 35^\circ C$ for the most probable hairpin structure).

DNA fragments corresponding to the genes of interest were amplified from genomic DNA using the established PCR conditions (9-11). For efficient binding to the sensor microarray probes, the DNA amplicon target must be single-stranded. Thus, the PCR amplicons were denatured at high temperature (95°C), and immediately injected into a measuring cell of an array. The disadvantage to this approach is that the second strand of the target amplicon is still present in the bulk solution, and can compete with the probes for target strand binding. However, this approach is attractive due to its simplicity and the absence of additional steps for single-stranded DNA target preparation.

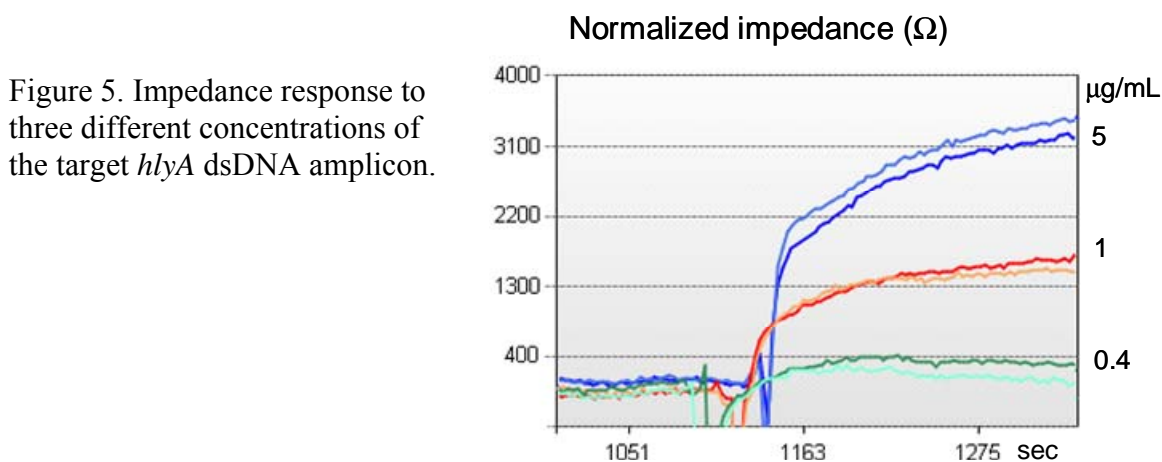


Figure 5 shows impedance responses obtained for three different concentrations of the *hlyA* double-stranded (ds) DNA amplicon. Clear dependence of the signal response on

the target concentration was observed. The strong impedance response was detected for 92 nM (5 µg/mL) concentration of the dsDNA amplicon, whereas the oligonucleotide targets produced a significant response starting from 600 nM concentrations (Fig. 4a). This difference in response to various target length (35 versus 355-mer for *hlyA* oligonucleotide and *hlyA* DNA amplicon, respectively) is consistent with impedance spectroscopy principles. Since the longer molecule contributes more negatively charged DNA phosphate backbone onto the electrode surface, it is detectable at lower concentrations (Fig. 4 and 5).

Similar to results with the oligonucleotide targets (Fig. 3), the impedimetric detection of dsDNA amplicons also demonstrated high specificity when non-target (negative control) and target amplicons were injected sequentially in the same cell. The typical exponential impedance response was observed only for injection of specific target amplicons (data not shown). Therefore, both sensitivity and specificity of impedimetric DNA assays are sufficient for detection of amplified bacterial DNA fragments of interest.

Conclusions

We have developed an integrated impedance spectroscopy platform applicable to a wide range of biological assays. The platform includes multiplexed sensor microarrays allowing a variety of bio-functionalizations, and a reader instrument capable of parallel detection of multiple electrode pairs using an integrated software package for data analysis. The platform performed well in nucleic acid assays, detecting specific binding of short oligonucleotides and DNA amplicon targets from different *E. coli* strains in real-time. Thus, the SLA platform fulfills our criteria for a simple, standardized sensing device providing integrated, real-time measurements of multiple biological targets in an array format.

References

1. F. Davis, M. A. Hughes, A. R. Cossins and S. P. Higson, *Anal. Chem.*, **79**, 1153 (2007).
2. G. P. Brewood, Y. Rangineni, D. J. Fish, A. S. Bhandiwad, D. R. Evans, R. Solanki, and A. S. Benight, *Nucleic Acid Res.*, **36**, e98 (2008).
3. A. Kukol, P. Li, P. Estrela, P. Ko-Ferrigno, and P. Migliorato. *Anal. Biochem.*, **374**, 143 (2008).
4. M. A. Vagin, S. A. Trashin, A. A. Karyakin, and M. Mascini, *Anal. Chem.*, **80**, 1336 (2008).
5. J. Weng, J. Zhang, H. Li, L. Sun, C. Lin, and Q. Zhang, *Anal. Chem.*, **80**, 7075 (2008).
6. A. L. Ghindilis, M. W. Smith, K. Schwarzkopf, C. Zhan, D. Evans, et al. *Electroanalysis*, **21**, 1459 (2009).
7. D. Bhaskar, D. Rao and K. S. Arun, *Proceedings of the IEEE*, **80**, 283 (1992).
8. R. Kumaresan and D. W. Tufts, *IEEE Trans. Acous. Speech, Sig. Proc.*, **30**, 833 (1982).
9. T. Wirth, D. Falush, R. Lan, F. Colles, P. Mensa, L. H. Wieler, H. Karch, P. R. Reeves, M. C. Maiden, H. Ochman, and M. Achtman, *Mol. Microbiol.*, **60**, 1136 (2006).
10. L. Beutin, S. Jahn, P. Fach, *J. Appl. Microbiol.*, **106**, 1122 (2009).
11. L. Beutin, G. Krause, S. Zimmermann, S. Kaulfuss, K. Gleier, *J. Clin. Microbiol.*, **42**, 1099 (2004).
12. S.-E. Fotinea, I. Dologlou, and G. Carayannis, *Int'l. J. Computer Maths. & Appl. (HERMIS-µπ)*, **8**, 84 (2006).